MI-836

Hard X-Ray Scanning Microscope at the ESRF Beamline ID 13

Final report

Jens Patommmel and Christian G. Schroer

Background of the project

The ESRF long-term project MI-836 was the continuation of the successful long-term project MI-704. The intention was to continue the development of a prototypical hard x-ray scanning microscope using nanofocusing refractive lenses at beamline ID 13 [Pat11]. In doing so, three major aims were persued. The first aim was to design, build and install the prototype and to demonstrate its performance by various experiments. The second aim was to provide a stable nanobeam that can be used for standard ESRF user experiments. The third aim was to use the experiences with the prototype in order to build an advanced nanoprobe instrument at the ESRF beamline ID 13 and elsewhere.

The scanning microscope was meant to operate with different x-ray analytical techniques like x-ray fluorescence analysis, absorption, and diffraction. In addition, the intention was to exploit the coherence of the focused beam to perform coherent x-ray diffraction imaging (CXDI) and x-ray ptychography. With a focus size of about 50 nm, a spatial resolution around 50 nm was expected for fluorescence element mapping and nano diffraction. The nanoprobe was designed to support two-dimensional mapping and tomographic techniques. Tomography would allow one to reconstruct the three-dimensional inner structure of specimens.

In consequence, the prototype instrument (Figure 1) was designed and built by the study group at TU Dresden, and it was installed and operated at the ESRF beamline ID 13. The prototype was not a long-time installation

at the beamline, but it had to be carried from Dresden to Grenoble and back for each experimental session. The exceptional effort was necessary to gain experience with nanofocus and microscopy techniques in view of a new nanoprobe at ID 13. In the later part of the long-term project, the beamline implemented its own nanoprobe permanently installed in experimental hutch 3 (EH 3). For this instrument, an optical module for nanofocusing lenses was designed and built at TU Dresden (Figure 2).

The nanoprobe project was supported by the German Department of Education and Research (BMBF).

The instrument at beamline ID 13

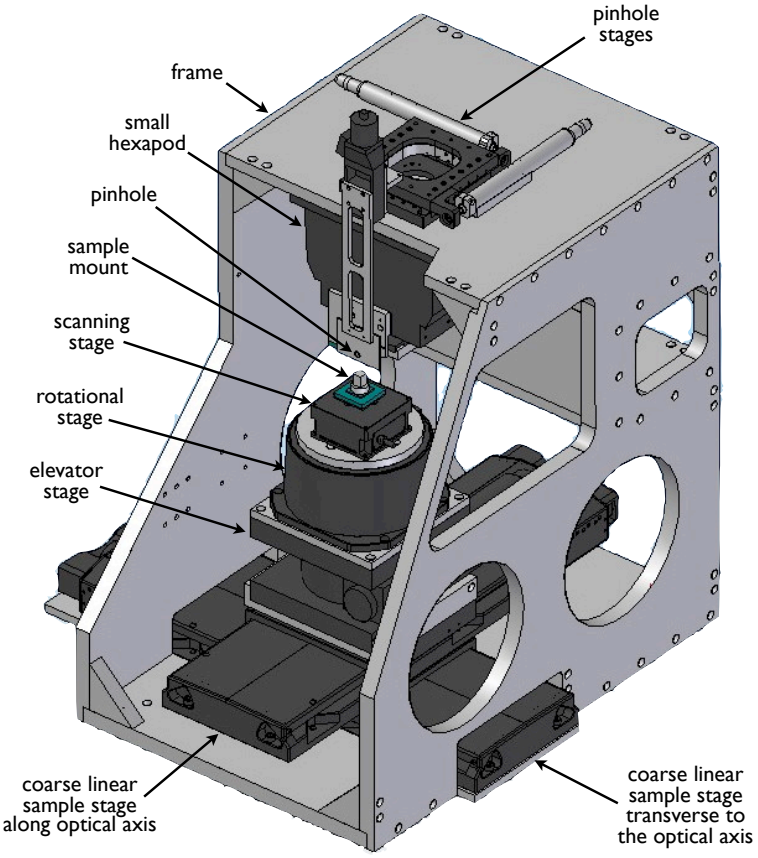

Figure 1: Schematic drawing of the prototypical nanoprobe version [Pat11].

Two setups were developed and used during the long-term project. On the one hand, there was the prototype nanoprobe completely built by TU

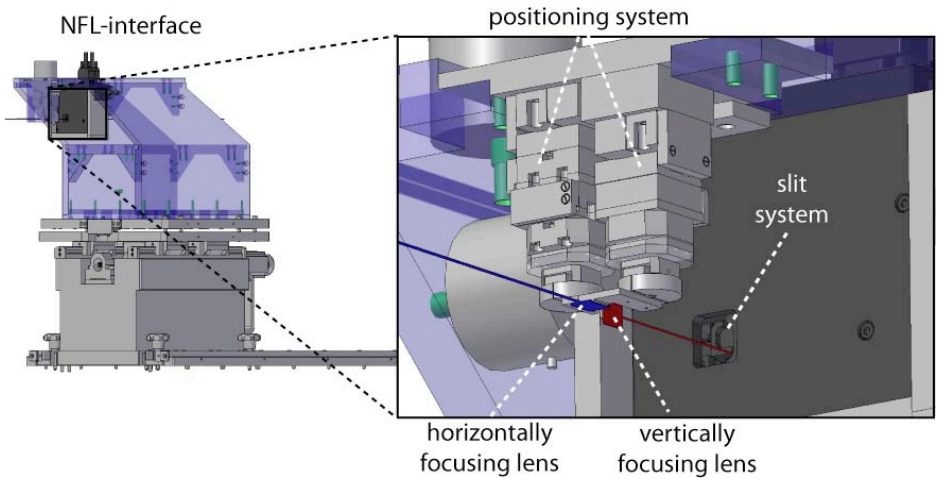

Figure 2: Permanently-installed nanoprobe with optics module designed and built by TU Dresen [Boy10].

Dresden and temporarily installed at the beamline (Fig. 1), and, on the other hand, an improved nanoprobe was used, which was permanently installed at the beamline ID 13 and for which the optics module for NFLs was delivered by TU Dresden within the project (Fig. 2). Both nanoprobes, the prototypical one and the permanent one, consist of a scanner unit including the sample module and the optics module firmly connected to guaranty stability.

For the new nanoprobe station at ID 13 the optics module contains the entry slits, the nanofocusing refractive lenses (NFLs), the pinhole, and all of the motorized stages to align these optical components.

Two-Stage Focusing

We developed a two-stage focusing scheme (Fig. 3) in order to adapt the coherence length to the effective aperture of the nanofocusing lenses. By this we were able to decide whether to have a highly coherent focus with limited flux or whether to decrease the coherence in the focus in favor of an increased photon flux. For fluorescence tomography, for example, coherence is not necessary, and the photon flux can be dramatically increased by using a prefocusing optic. For CXDI and ptychography, however, a large coherence length is required and the prefocusing lenses would be adapted, accordingly.

At beamline ID 13, several compound parabolic refractive lenses made of beryllium (CRLs) are installed and ready to be used whenever needed. There are white-beam lenses between the undulator and the monochromator, and there are CRLs between the monochromator and the nanoprobe provided by

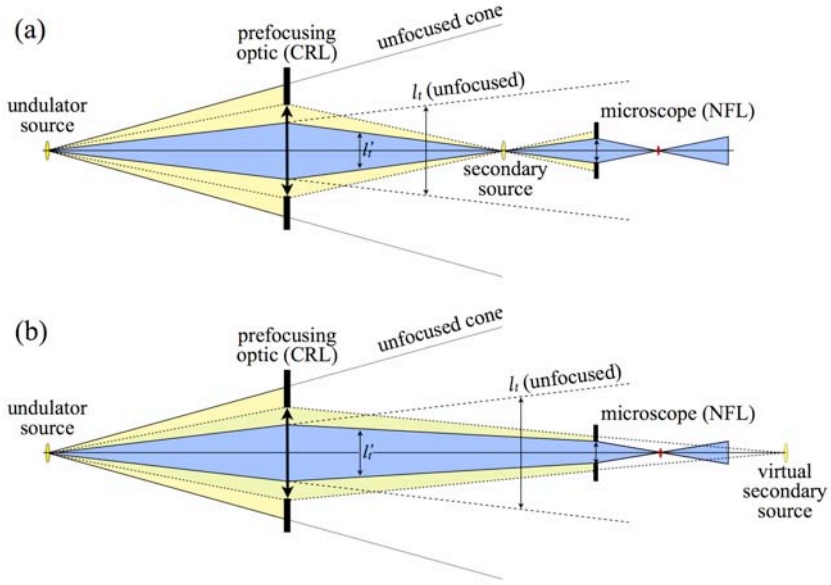

Figure 3: Two-stage focusing scheme. (a) Real secondary source between prefocusing optic and NFL. (b) Virtual secondary source behind nanofocusing lens. (From [Pat11].)

TU Dresden. We performed series of tests with different prefocusing geometries and parameters and we found that the photon flux could be increased by a factor of ∼20, while the focus size increased by a factor of ∼1.5, only.

Experimental sessions

In the course of the long-term project, four experimental sessions were scheduled as shown in table 1.

In the first session, the prototype was installed in experimental hutch 2 (EH 2), while in all the other sessions, the permanently-installed nanoprobe in EH 3 was used in combination with the TUD optics module.

Fluorescence element mapping

X-ray fluorescence analysis is one of the major x-ray analytical techniques performed with the scanning microscope. In case of thin samples, the specimens can be investigated with two-dimensional element mapping, scanning the sample laterally in two dimensions with the focused beam. At each scanning position, the fluorescence spectrum is recorded with an energy-dispersive detector, from which the two-dimensional projected element distribution can

Session	Begin	End	Topic
MI-836.1	2008 Feb 7th	2008 Mar 4th	Fluorescence tomography of a pollen CXDI with 100 nm gold particles
MI-836.2	2009 Feb 25th	2009 Mar 4th	CXDI with 50 nm gold particles Fluorescence mapping of interfaces Test of NFLs made from diamond
MI-836.3/4	2009 Jun 29th	2009 Jul 21st	CXDI with 20 nm gold particles CXDI tomography with gold particles Ptychography for beam characterization
MI-836.5	2010 Feb 13th	20010 Mar 17th	Defocused ptychography Ptychography of a micro chip

Table 1: Experimental sessions.

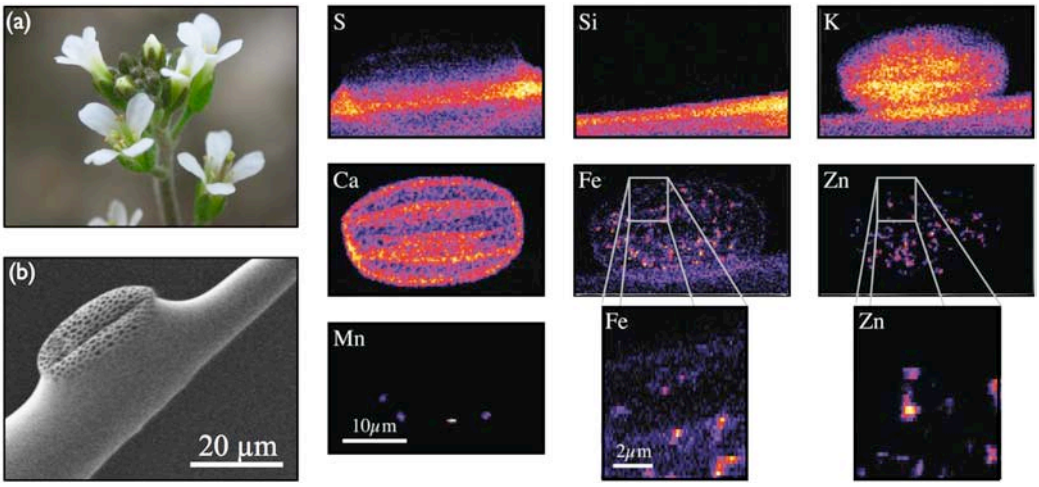

Figure 4: Fluorescence element mapping of the pollen of *Arabidopsis thaliana*. (a) Photograph of an *Arabidopsis thaliana* plant. (b) SEM image of the pollen of *Arabidopsis thaliana*. (right) Measured element distribution retrieved from the fluorescence signal. Resolved features range down to the size of only 1 or 2 pixels, which corresponds to a spatial resolution of about 100 nm.

be retrieved. X-ray fluorescence element mapping is especially useful for extremely low concentration of elements, that is for example often the case of micronutrients inside biological samples. We applied this method not only to biological specimens, but also to cosmic particles, Stranski-Krastanow islands [HDS$^+$08, DHS$^+$10], geological samples, and many more.

Figure 4 shows the result of x-ray fluorescence element mapping of a pollen of *Arabidopsis thaliana* carried out during the experimental session MI-836.2. The element distribution maps are given with a spatial resolution

of better than 100 nm.

Fluorescence tomography

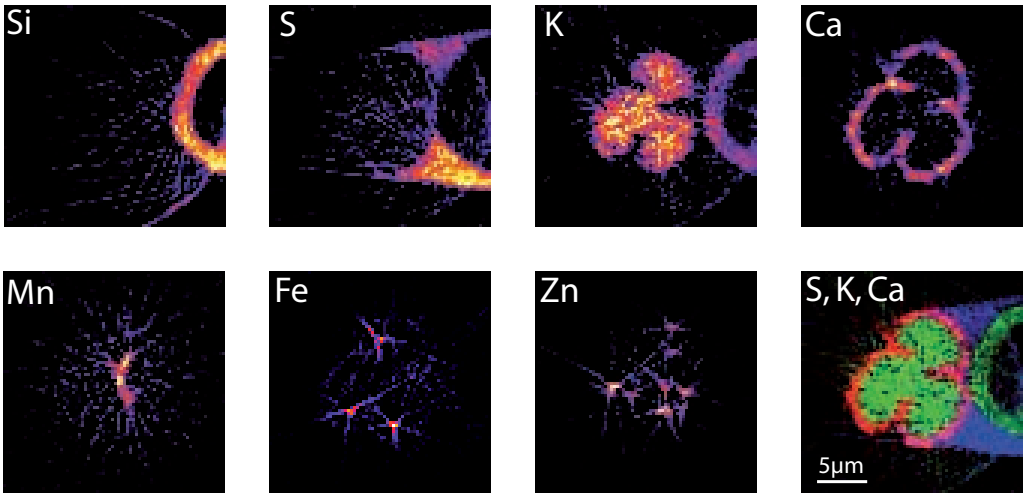

Figure 5: Reconstructed element distribution of the pollen of *Arabidopsis thaliana* retrieved from the tomogram of the fluorescence signal. The specimen is the same as seen in Figure 4.

Fluorescence element mapping reveals the two-dimensional element distribution in a sample projected along the optical axis. This is sufficient for thin samples, but in case of samples extended in three dimensions, the information loss due to projecting is not admissible and tomographic techniques must be applied. The hard x-ray scanning microscope is furnished with a high precision rotational stage with air bearing that allows for tomography with high spatial resolution.

Figure 5 depicts a reconstructed tomographic slice with distributions for various elements of the pollen of *Arabidopsis thaliana* as the result of a tomogram. The sample is the same as the one in Figure 4. In contrast to the two-demensional element mapping method described in the previous section, this tomographic experiment delivers information about whether a structure is located in the inner or rather in the outer region of the specimen. This example demonstrates the necessary of applying tomographic methods for inhomogeneous three-dimensional objects. The experiment was carried out in experimental session MI-836.2.

Coherent x-ray diffraction imaging (CXDI)

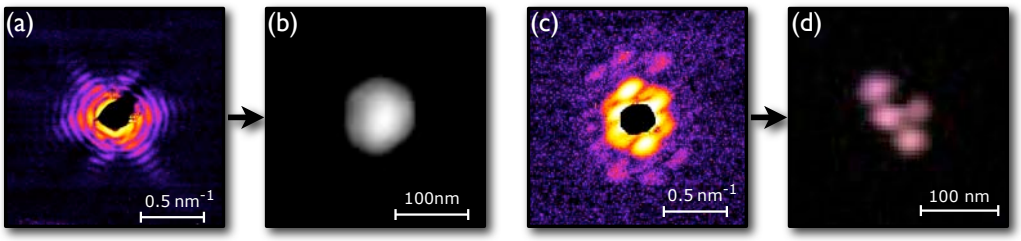

Figure 6: Coherent x-ray diffraction imaging with gold particles. (a) This diffraction pattern of a 100 nm gold particle was used to reconstruct the electron density shown in (b) [SBF$^+$08]. (c) The diffraction pattern of a cluster of 4 gold particles with 50 nm diameter was used to reconstruct the electron density shown in (d) [SBF$^+$10a].

The hard x-ray scanning microscope generates a highly coherent focal spot that can be used for coherent x-ray diffraction imaging (CXDI) [MCKS99, CBM$^+$06, STB$^+$05] and for ptychography [RF04, RHC$^+$07, TDM$^+$08]. In a CXDI experiment, an object is completely illuminated by an x-ray beam and the diffraction pattern behind the sample is recorded with sufficient sampling. The diffraction pattern, together with some knowledge about the illumination allows one to reconstruct the transmission function of the object. In this method, the resolution is not given by the numerical aperture of an x-ray optic, but by the largest scattering angle that contains observable scattering signal, and, therefore, by the coherent photon dose seen by the object [SBF$^+$08, SS10]. In order to reduce the exposure time, a high coherent flux is needed, and thus, focusing the coherent flux of a given source onto the specimen is crucial for CXDI.

Figure 6 shows the results of two CXDI experiments with gold particles [SBF$^+$08, SBF$^+$10a]. Figures 6(a) and (b) refer to a single gold particle with 100 nm diameter and 6(c) and (d) refer to a cluster of four gold particles with 40 nm diameter. The achieved spatial resolution was 5 nm [SBF$^+$08]. To achieve this, the sample was exposed for 10 minutes. Without focusing the coherent flux onto the sample, the total exposure time would have to be more than two months in order to gain the same spatial resolution. This CXDI experiment was pioneering in several ways. It was for the first time that CXDI was successfully performed with x-rays with wavelength below 1 Å without using a Bragg reflexion of a crystalline sample. Besides that, we demonstrated a spatial resolution of below 10 nm, which had never been achieved before.

Ptychography

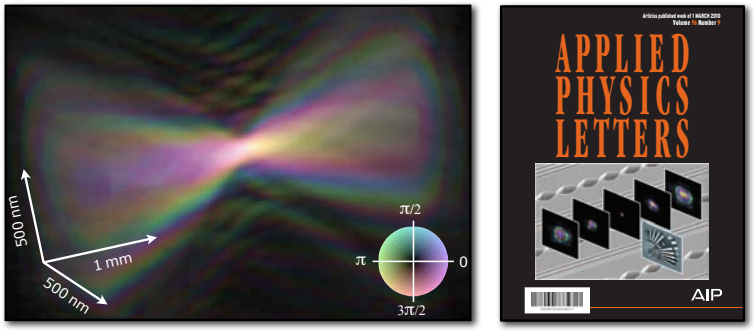

Figure 7: Ptychography for beam characterization. The complex wavefield (phase and amplitude) around the focal plane was reconstructed by means of ptychography [SBF$^+$10b].

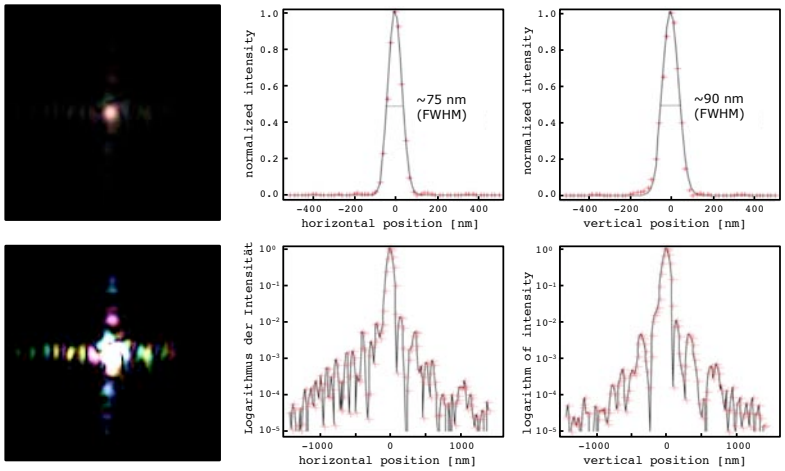

Figure 8: Line profile through the complex wavefield in the focal plane [SBF$^+$10b].

In the course of the long-term project, it became more and more apparent, that ptychography would be one of the most important techniques provided by the nanoprobe. Ptychography, in contrast to CXDI, needs no information about the illumination. It even quantitively reveals the complex illumination function in the object plane, and thus the complete caustic of the nanobeam. In addition, the object is reconstructed without ambiguity, which is not the case for CXDI. Another advantage of ptychography over CXDI is the possibility to investigate samples that are larger than the illumination [TDM$^+$08, TDB$^+$09, MR09, GSF09].

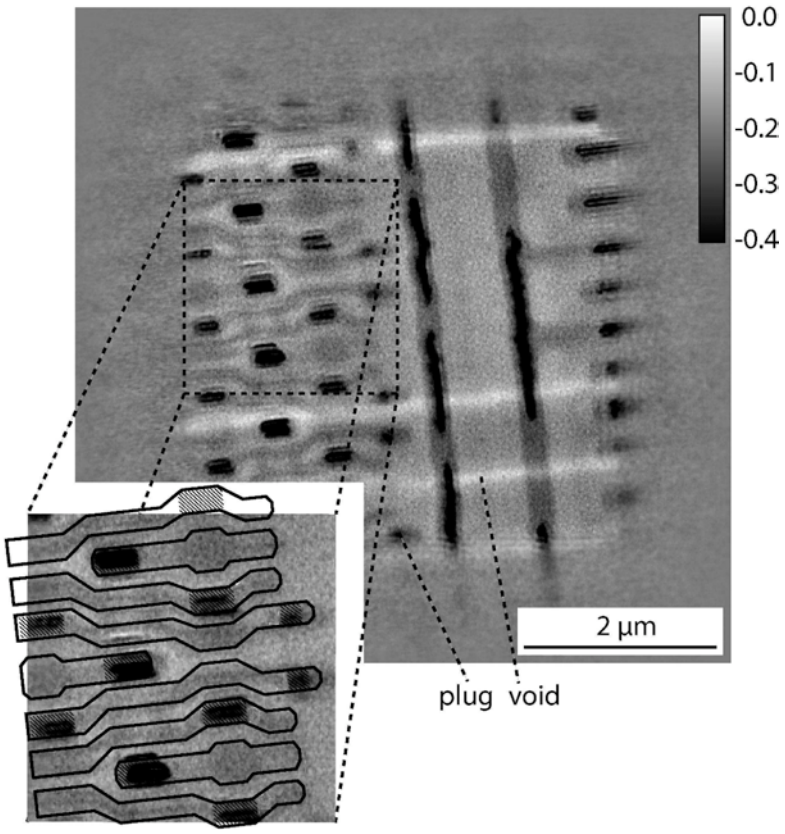

Figure 9: Reconstructed phase of a microchip retrieved from a ptychography experiment [SBG+11].

In a ptychography experiment, the specimen is scanned with the coherent x-ray beam with sufficient overlap between neighboring scan points. At each scan point the diffraction pattern is recorded with appropriate sampling. From the set of diffraction patterns, the complex illumination function in the object plane can be reconstructed as well as the complex transmission function of the object. By Fresnel propagation of the wavefield, the complete caustic of the nanobeam can be retrieved.

We performed the first successful ptychography scan during the experiment session MI-836.3 in the summer of 2009. While the spatial resolution of the reconstructed object was still suboptimal due to mechanical instabilities, the beam was characterized with a precision never achieved before. We published this new method for nanobeam characterization in applied physics letters (Figure 7) [SBF+10b]. Figure 8 shows the line profile through the focal plane of the nanoprobe. The beam size of 75 nm by 90 nm conforms with the resolution of the fluorescence map that was recorded in parallel with

the ptychography scan. The intensity outside the central speckle of the focus is smaller by a factor of 100 compared to the maximum. This demonstrates the high quality of the focus generated by the nanofocusing lenses made of silicon.

We used a generic sample (NTT test pattern made of tungsten) for beam-charecterization by ptychography. In addition to that, we also investigated further samples like, for example, a memory chip. Figure 9 shows the reconstructed phase of a microchip which was probed in a ptychography scan [SBG+11]. This is a first example of high resolution hard x-ray microscopy of a buried structure that could not be achieved by other microscopy methods without sample destruction.

Nanofocusing Lenses

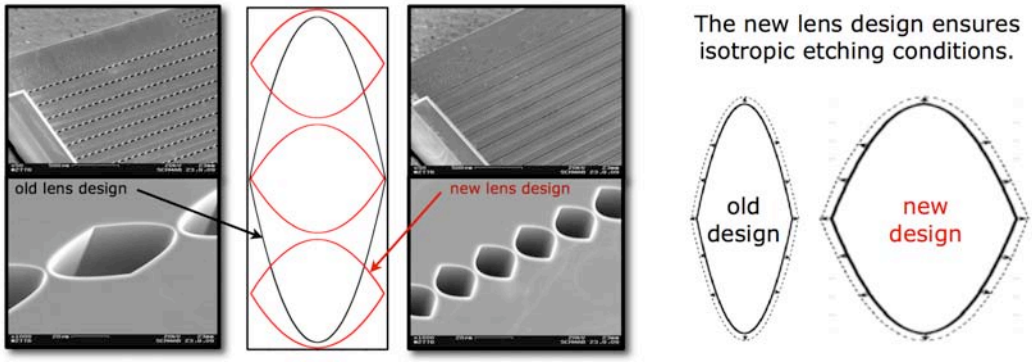

Figure 10: New lens design for the nanofocusing lenses [Boy10].

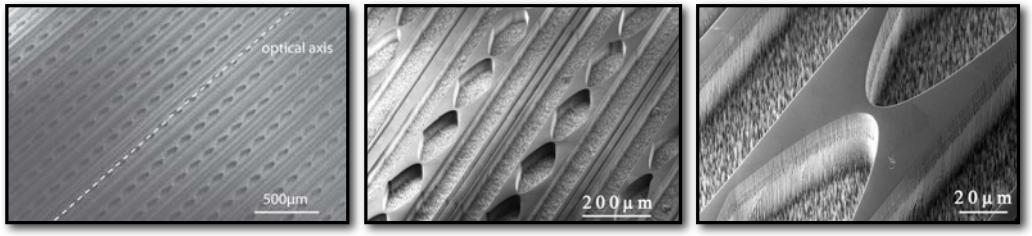

Figure 11: SEM images of nanofocusing lenses made from diamond [Boy10].

The hard x-ray scanning microscope uses nanofocusing lenses made from silicon to generate the nanobeam. Applying ptychography, the nanoprobe

allows to reconstruct the caustic of the nanobeam (see section "Ptychography"). This feedback information is used to learn about aberrations of the NFLs and to improve the lenses. One important insight was that a more isotropic lens shape reduces aberrations due to isotropic etching conditions during lens fabrication (Figure 10). During the long-term project, the nanofocusing lenses could be improved with regards to steepness of the sidewalls, surface roughness, and shape contour accuracy thus reducing spherical aberrations [BFP+09, Boy10].

Silicon is not the optimal lens material with regards to x-ray transmission, refractive power, and thus efficiency and diffraction limit. The reason for choosing silicon as lens material is the availability of established technological processes, which allow the fabrication of nearly aberration free lens structures. Lens materials with better x-ray optical properties are, for example, boron and diamond. The fabrication of lenses made from boron or diamond is quite difficult, and, until now, there are no refractive lenses made of boron or diamond with shape accuracy, low surface roughness, and depth of lens structures, which are even nearly as good as for silicon.

Despite the technological challenges, our study group in Dresden cooperates with Diamond Materials in Freiburg, Germany, with the intention to establish a process for producing refractive diamond lenses. First lenses were fabricated in 2009 (Fig. 11), and we tested these diamond lenses with the nanoprobe setup in experiment session MI-836.2. A focus of size 360 nm FWHM could be generated by the diamond lenses, which was demonstrated by knife-edge scans. There are still strong aberrations of the lens shape, and the depth of the lens structures has to be further increased. For future experiments, improved diamond lenses will be available and tested with the scanning microscope.

User Support

The experimental sessions of the long-term project were combined with user experiments, which had been proposed by user groups not involved in the long-term project MI-836. The procedure was that we started our sessions with the installation of the prototype or of the optics module, respectively, followed by the alignment of the nanofocusing lenses. Once the nanoprobe was aligned, it could be used for experiments. On the one hand, we performed our own experiments as exemplified in the preceding paragraphs. On the other hand, third-party users came along and, with our support, executed their experiments with the hard x-ray scanning microscope. The third-party user experiments are shown in table 2

Date	User	Topic
Feb 2008	Vince, et al.	Stardust
Feb 2008	Als-Nielsen, et al.	Fluorescence of iron structures
Feb 2008	Hanke, et al.	Si/Ge islands
Mar 2009	Hanke, et al.	Si/Ge islands
Jul 2009	Salditt, et al.	Coherent scattering experiments
Feb 2010	Faidenhans'l , et al.	Coherent scattering experiments
Feb 2010	Vince, et al.	Stardust
Mar 2010	Hanke, et al.	Si/Ge islands

Table 2: User support.

Publications Resulting From This Long-Term Project

[1] Andreas Schropp, Pit Boye, Andy Goldschmidt, Susi Hönig, Robert Hoppe, Jens Patommel, Christoph Rakete, Dirk Samberg, Sandra Stephan, Sebastian Schöder, Manfred Burghammer, and Christian G. Schroer. Non-destructive and quantitative imaging of a nano-structured microchip by ptychographic hard x-ray scanning microscopy. *Journal of Microscopy*, 241(1):9–12, 2011.

[2] Andreas Schropp, Pit Boye, Jan M. Feldkamp, Robert Hoppe, Jens Patommel, Dirk Samberg, Sandra Stephan, Klaus Giewekemeyer, Robin N. Wilke, Tim Salditt, Johannes Gulden, Adrian P. Mancuso, Ivan A. Vartanyants, Edgar Weckert, Sebastian Schöder, Manfred Burghammer, and Christian G. Schroer. Hard x-ray nanobeam characterization by coherent diffraction microscopy. *Appl. Phys. Lett.*, 96(9):091102, 2010.

[3] M. Dubslaff, M. Hanke, S. Schoeder, M. Burghammer, T. Boeck, and J. Patommel. X-ray nanodiffraction at individual SiGe/Si(001) dot molecules and its numerical description based on kinematical scattering theory. *Appl. Phys. Lett.*, 96(13), March 2010.

[4] C. G. Schroer, P. Boye, J. M. Feldkamp, J. Patommel, A. Schropp, D. Samberg, S. Stephan, M. Burghammer, S. Schöder, C. Riekel, B. Lengeler, G. Falkenberg, G. Wellenreuther, M. Kuhlmann, R. Frahm, D. Lützenkirchen-Hecht, and W. H. Schroeder. Hard X-ray microscopy with elemental, chemical, and structural contrast. *Acta Physica Polonica A*, 117(2):357–368, 2010.

[5] Pit Boye, Jan M. Feldkamp, Jens Patommel, Andreas Schwab, Sandra Stephan, Robert Hoppe, Christian G. Schroer, Manfred Burghammer, Christian Riekel, Andre van der Hart, and Matthias Küchler. Nanofocusing refractive x-ray lenses: Fabrication and modeling. In *9th International Conference on X-ray Microscopy*, volume 186 of *Journal of Physics: Conference Series*, page 012063, 2009.

[6] Christian G. Schroer, Pit Boye, Jan M. Feldkamp, Jens Patommel, Andreas Schropp, Andreas Schwab, Sandra Stephan, Manfred Burghammer, Sebastian Schöder, Christian Riekel, and Walter H. Schröder. Hard x-ray scanning microscopy with fluorescence and diffraction contrast. In *9th*

International Conference on X-ray Microscopy, volume 186 of *Journal of Physics: Conference Series*, page 012016, 2009.

[7] M. Hanke, M. Dubslaff, M. Schmidbauer, T. Boeck, S. Schöder, M. Burghammer, C. Riekel, J. Patommel, and C. G. Schroer. Scanning x-ray diffraction with 200 nm spatial resolution. *Appl. Phys. Lett.*, 92(19):193109, Jan 2008.

[8] Christian G. Schroer, Pit Boye, Jan Feldkamp, Jens Patommel, Andreas Schropp, Andreas Schwab, Sandra Stephan, Manfred Burghammer, Sebastian Schöder, and Christian Riekel. Coherent x-ray diffraction imaging with nanofocused illumination. *Phys. Rev. Lett.*, 101(9):090801, 2008.

[9] Christian G. Schroer, Pit Boye, Jan M. Feldkamp, Jens Patommel, Andreas Schropp, Andreas Schwab, Sandra Stephan, Manfred Burghammer, Sebastian Schöder, and Christian Riekel. Coherent x-ray diffraction imaging with nanofocused illumination. *Virtual Journal of Nanoscale Science & Technology*, 18(10), 2008.

References

[BFP+09] Pit Boye, Jan M. Feldkamp, Jens Patommel, Andreas Schwab, Sandra Stephan, Robert Hoppe, Christian G. Schroer, Manfred Burghammer, Christian Riekel, Andre van der Hart, and Matthias Küchler. Nanofocusing refractive x-ray lenses: Fabrication and modeling. In *9th International Conference on X-ray Microscopy*, volume 186 of *Journal of Physics: Conference Series*, page 012063, 2009.

[Boy10] Pit Boye. *Nanofocusing Refractive X-Ray Lenses*. PhD thesis, Technical University of Dresden (TU Dresden), 2010. urn:nbn:de:bsz:14-qucosa-27137, http://nbn-resolving.de/urn:nbn:de:bsz:14-qucosa-27137.

[CBM+06] Henry N. Chapman, Anton Barty, Stefano Marchesini, Aleksandr Noy, Stefan P. Hau-Riege, Congwu Cui, Malcolm R. Howells, Rachel Rosen, Haifeng He, John C. H. Spence, Uwe Weierstall, Tobias Beetz, Chris Jacobsen, and David Shapiro. High-resolution ab initio three-dimensional x-ray diffraction microscopy. *J. Opt. Soc. Am. A*, 23(5):1179–1200, Jan 2006.

[DHS+10] M. Dubslaff, M. Hanke, S. Schoeder, M. Burghammer, T. Boeck, and J. Patommel. X-ray nanodiffraction at individual SiGe/Si(001) dot molecules and its numerical description based on kinematical scattering theory. *Appl. Phys. Lett.*, 96(13), March 2010.

[GSF09] Manuel Guizar-Sicairos and James R. Fienup. Measurement of coherent x-ray focused beams by phase retrieval with transverse translation diversity. *Opt. Express*, 17(4):2670–2685, 2009.

[HDS+08] M. Hanke, M. Dubslaff, M. Schmidbauer, T. Boeck, S. Schöder, M. Burghammer, C. Riekel, J. Patommel, and C. G. Schroer. Scanning x-ray diffraction with 200 nm spatial resolution. *Appl. Phys. Lett.*, 92(19):193109, Jan 2008.

[MCKS99] Jianwei Miao, Pambos Charalambous, Janos Kirz, and David Sayre. Extending the methodology of X-ray crystallography to allow imaging of micrometre-sized non-crystalline specimens. *Nature*, 400:342–344, 1999.

[MR09] Andrew M Maiden and John M Rodenburg. An improved ptychographical phase retrieval algorithm for diffractive imaging. *Ultramicroscopy*, 109(10):1256–1262, Jan 2009.

[Pat11] Jens Patommel. *Hard X-Ray Scanning Microscope Using Nanofocusing Parabolic Refractive Lenses*. Cuvillier Verlag Göttingen, 1st edition, January 2011. PhD theses, ISBN 978-3-86955-614-7.

[RF04] J. M. Rodenburg and H. M. L. Faulkner. A phase retrieval algorithm for shifting illumination. *Appl. Phys. Lett.*, 85(20):4795–4797, 2004.

[RHC+07] J. M. Rodenburg, A. C. Hurst, A. G. Cullis, B. R. Dobsen, F. Pfeiffer, O. Bunk, C. David, K. Jefimovs, and I. Johnson. Hard-x-ray lensless imaging of extended objects. *Phys. Rev. Lett.*, 98:034801, 2007.

[SBF+08] Christian G. Schroer, Pit Boye, Jan Feldkamp, Jens Patommel, Andreas Schropp, Andreas Schwab, Sandra Stephan, Manfred Burghammer, Sebastian Schöder, and Christian Riekel. Coherent x-ray diffraction imaging with nanofocused illumination. *Phys. Rev. Lett.*, 101(9):090801, 2008.

[SBF+10a] C. G. Schroer, P. Boye, J. M. Feldkamp, J. Patommel, A. Schropp, D. Samberg, S. Stephan, M. Burghammer, S. Schöder, C. Riekel, B. Lengeler, G. Falkenberg, G. Wellenreuther, M. Kuhlmann, R. Frahm, D. Lützenkirchen-Hecht, and W. H. Schroeder. Hard X-ray microscopy with elemental, chemical, and structural contrast. *Acta Physica Polonica A*, 117(2):357–368, 2010.

[SBF+10b] Andreas Schropp, Pit Boye, Jan M. Feldkamp, Robert Hoppe, Jens Patommel, Dirk Samberg, Sandra Stephan, Klaus Giewekemeyer, Robin N. Wilke, Tim Salditt, Johannes Gulden, Adrian P. Mancuso, Ivan A. Vartanyants, Edgar Weckert, Sebastian Schöder, Manfred Burghammer, and Christian G. Schroer. Hard x-ray nanobeam characterization by coherent diffraction microscopy. *Appl. Phys. Lett.*, 96(9):091102, 2010.

[SBG+11] A. Schropp, P. Boye, A. Goldschmidt, S. Hönig, R. Hoppe, J. Patommel, C. Rakete, D. Samberg, S. Stephan, S. Schöder, M. Burghammer, and C. G. Schroer. Non-destructive and

quantitative imaging of a nano-structured microchip by ptychographic hard x-ray scanning microscopy. *Journal of Microscopy*, 241(1):9–12, 2011.

[SS10] Andreas Schropp and Christian G. Schroer. Dose requirements for resolving a given feature in an object by coherent x-ray diffraction imaging. *New Journal of Physics*, 12:035016, 2010.

[STB+05] D. Shapiro, P. Thibault, T. Beetz, V. Elser, M. Howells, C. Jacobsen, J. Kirz, E. Lima, H. Miao, A. M. Neiman, and D. Sayre. Biological imaging by soft x-ray diffraction microscopy. *P. Natl. Acad. Sci. USA*, 102:15343–15346, Jan 2005.

[TDB+09] Pierre Thibault, Martin Dierolf, Oliver Bunk, Andreas Menzel, and Franz Pfeiffer. Probe retrieval in ptychographic coherent diffractive imaging. *Ultramicroscopy*, 109(4):338–343, 2009.

[TDM+08] Pierre Thibault, Martin Dierolf, Andreas Menzel, Oliver Bunk, Christian David, and Franz Pfeiffer. High-resolution scanning x-ray diffraction microscopy. *Science*, 321(5887):379–382, 2008.